

Effect of Radial Pressure and Lubricant Types on Partial Discharge Inception in a Slip-On Medium Voltage XLPE Cable Termination

Emre KANTAR, Sverre HVIDSTEN, Jørund AAKERVIK; SINTEF Energy Research, Norway,
Emre.Kantar@sintef.no, Sverre.Hvidsten@sintef.no, Jorund.Aakervik@sintef.no

ABSTRACT

The most critical section in a cable termination or a subsea connector is the interface between the cable surface and the inner surface of the termination body, including the semiconductive geometric field grading. Partial discharge (PD) measurements were performed on a commercial 24 kV slip-on termination installed on a 12-kV XLPE cable, including two different lubricants and two additional external radial pressures, using an insulating vulcanization (IV) rubber tape. The results indicated that increasing the total radial pressure above the nominal level obtained when expanding the termination on the cable core resulted in a higher PD inception voltage independent of the lubricant type. It is also likely that the higher viscosity of the lubricant increased the PD inception voltage of the termination at the same interfacial stress and surface roughness.

KEYWORDS

Cable termination, inception, interfacial pressure, insulating liquid, lubricant, partial discharge.

INTRODUCTION

In recent years, the global rise in demand for renewable energy has led to a significant expansion of offshore wind farms. For offshore wind power, submarine power cable systems (including components such as connectors and terminations) play a crucial role in transmitting power to the shore. However, evidence from the past two decades showed that power cables and connectors have emerged as the primary factor contributing to power supply failures in offshore plants [1]. Despite significant advancements in material science and manufacturing processes, one persisting challenge is the vulnerability of solid-solid interfaces within the cable systems, where the surfaces of two different solid materials come into direct contact [2]. The contacts occur at discrete spots, resulting in a myriad of sub-microcavities and channels forming between adjacent contact points at the interface [3]. Partial discharges (PDs) can occur in the microcavities at the interface at a certain stress level, which may, over time, lead to insulation degradation, increase the risk of electrical breakdown and failure, and thus reduce service life [4].

These interfaces can be found between cable insulation and rubber stress cones in joints and terminations or between rubber stress cones and epoxy components in joints [5]. The most critical section is the interface between the cable and the semiconductive geometric field grading material, as illustrated in the highlighted area ④ in Fig. 1.

The electrical breakdown strength of the interface strongly depends on the interfacial pressure. Surface roughness, elastic modulus, type of lubricant, and temperature change are the other factors that affect the interfacial breakdown strength because they all significantly affect the dielectric properties of sub-microcavities and channels [6]–[8].

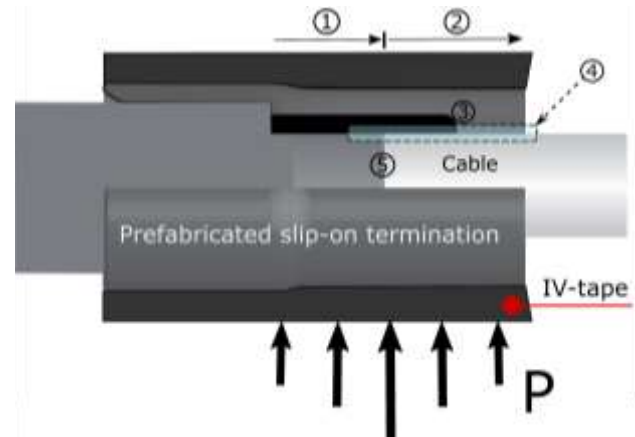


Fig. 1: Illustration of the cable-termination interface. Axial section with 1: no electrical stress outside cable/connector, 2: high electrical stress outside cable/connector. 3: Electrical field grading. 4: Interface between the SOT and cable. 5: End cut of the insulation screen of the cable. P: Uniform radial external pressure on the SOT using insulating vulcanization (IV) tape.

To obtain the needed interfacial pressure, the elasticity (i.e., intrinsic radial pressure) of the rubber body is normally utilized when expanded on a cable core. Three main factors that control the interfacial pressure are elastic modulus, strain, and wall thickness of the rubber termination material. Applying an additional external radial pressure on the termination could increase the inception and extinction voltage of PDs (PDIV and PDEV). Until now, this has not been utilized in terminations or connectors. It is important that the rubber material is retained within its elastic region when applying external pressure; otherwise, plastic deformation will cause dislocations within the material and a permanent change in shape [3]. Furthermore, apart from its dielectric properties, the viscosity of the lubricant present at the interface also becomes a key parameter influencing the PDIV/PDEV in the presence of external radial pressure (see ④ in Fig.1).

The main purpose of this paper is to study the effect of interfacial pressure and insulating liquid types on the partial discharge inception voltage of a silicone rubber (SiR) type slip-on cable termination (SOT).

EXPERIMENTAL WORK

Assembly of test objects

A 6/10 (12) kV XLPE-insulated cable, with a 120 mm² cross-section, 3.9 mm insulation thickness, and a fully bonded insulation screen, was used. The sections in contact with the rubber terminations were peeled and polished prior to installation, as illustrated in Fig. 1. The polishing was done using the back side of a 400-grit sandpaper. The SiR outdoor SOT terminations, designed

for a maximum system voltage (U_m) of 24 kV, were installed on both cable ends following the completion of cable preparation. The SOT has a semiconductive field grading, as illustrated in Fig. 1. Prior to installation, the lengths of the terminations were reduced by removing their sheds. The polishing was repeated each time a new SOT was installed using the same cable core and following the same procedure. The surface profiles of the peeled and polished surfaces were measured using a 3D optical profiler (Bruker Contour GT-K) in the vertical scanning interferometry mode. Each scan had a surface area of 1.25 mm × 0.94 mm. The arithmetic mean height (S_a), mean spacing of profile irregularities (S_m), and surface material volume (S_{mv}) of the unpolished and polished surfaces were calculated using Bruker's Vision64 software.

Test procedure

Two different lubricants, namely, a silicone grease and a synthetic ester, were used while installing the SOTs on the cable core. Their basic properties are shown in Table 1. External radial pressure at the interface between the SOT and XLPE cable surfaces was applied by wrapping insulating vulcanization (IV) rubber tape over the SOTs, as illustrated in Fig. 1. Three different pressure levels were applied to the SOT after assembling it in compliance with the installation guide: i) No additional pressure except for the nominal pressure of the expanded SOT over the cable core, ii) Medium pressure where the IV tape was stretched nominally during installation, iii) High pressure where the IV tape was wrapped around the SOTs with maximum stretching. Wrapping of the IV tape was performed with a staggering of around 50% from one layer to the next, and there were, in total, six layers wrapped over the SOT for the cases of medium and high pressure. Note that the actual resulting interfacial pressure was not measured nor calculated in this work. The SOT body was moved along the cable core into position according to the installation guide when using the silicone grease as the lubricant. In the case of synthetic ester, the SOT was initially positioned on a polymeric support prior to moving it into position over the end cut of the insulation screen, as illustrated in Fig. 1.

Test objects prepared in a sequence are shown in Table 2. The same cable core was used each time. Initially, the high pressure and silicone grease were applied to both cable terminations (test object no. 1). Then, one of the SOTs was removed and replaced with a new SOT, which was subjected to the pressure magnitude and lubricant type, as indicated in Table 2. The other SOT was kept as initially installed during the complete test sequence (test object no. 1-6). Prior to each installation, the surface of the XLPE at sections close to the end cut of the insulation screen was polished as previously explained to remove any marks from PD activity/ageing of the previous test.

Table 1: Properties of the lubricants.

Property	Silicone grease	Synthetic ester [9]
AC Dielectric breakdown field (kV/mm)	> 20 [10]	> 30
Relative permittivity (at 30°C)	~ 2.5 [10]	~ 3.2
Volume resistivity (Ohm.cm at 90°C)	2×10^{11} [11]	$> 20 \times 10^{11}$
Viscosity (mm ² /s)	1000 [11]	29

Table 2: Test objects prepared in a sequence.

Test object no.	External pressure magnitude	Lubricant type
1	High (baseline)	Silicone grease
2	Medium	Silicone grease
3	None (reference)	Silicone grease
4	High	Synthetic ester
5	Medium	Synthetic ester
6	None	Synthetic ester

PD measurements

PD measurements were performed according to IEC 60270 where the amplitude spectrum was integrated with a center frequency of 250 kHz and a bandwidth of 300 kHz. The PD detection threshold/PD sensitivity was set to 0.8 pC during the tests. A commercially available measurement impedance from Omicron, CPL542, was connected to the data processing unit MPD 600 to record the PD signals.

The cable terminations (SOTs) were submerged in plastic containers filled with the same synthetic ester used as a lubricant to avoid external flashover. The cable and SOTs were energized with a 50 Hz AC voltage at 10 kV (rms). The voltage was then increased in $\Delta V = 2$ kV voltage steps, with each step applied for $\Delta t = 5$ min. The voltage was increased until continuous PD signals were detected, as illustrated in Fig. 2. The voltage value at which repetitive PDs originate from the interface (noise-free > 0.8 pC) was recorded as the PDIV for the tested object, in accordance with IEC 60270. The baseline PDIV, obtained under high pressure with grease (test object no. 1), was presumed to yield the highest PDIV. Thus, if the PDIV of the newly tested SOT was lower than the baseline PDIV value, this value was recorded as the PDIV for the tested SOT. The SOT-cable system was subjected to the PDIV magnitude for 5 minutes according to test protocol unless the repetitive discharge magnitudes exceeded 100 pC. Then, the voltage started to be decreased at the same rate and kept for the same duration, as displayed in Fig. 2, until the PDs were quenched (PD extinction voltage-PDEV). It should be noted that bursts of momentary discharges were not considered as the PDIV value unless they occurred repetitively during the entire period.

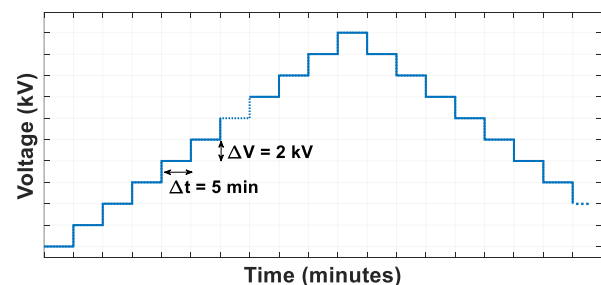


Fig. 2: Applied voltage to measure PDIV, PDEV, and PD-related quantities for the SOTs.

Phase-Resolved PD (PRPD) plots were used to display the raw PD data, where each PD event is resolved into the apparent discharge magnitude (Q_a), phase angle (φ), and the number of PDs (n). The PD data were exported from the Omicron software to MATLAB in binary format to plot PRPD figures and derive several PD quantities following

the guidelines in IEC 60270, such as the number of discharges, average and maximum discharge magnitudes, and total measured apparent charge during a voltage period. We excluded PD magnitudes above the 99.9th percentile in the analysis to eliminate outliers.

RESULTS

Surface characterization

Fig. 3(a) presents the cable surface after peeling the bonded semiconductor material. The marks from the cutting tool are visible in repeating patterns. The part of the cable surface in contact with the SOT (see ④ in Fig. 1) was polished, as displayed in Fig. 3(b). The polished surface seems to be notably smoother. Fig. 3(c) and (d) illustrate the 3D surface profiles, showcasing exemplary peak-to-valley heights between the cursors. The unpolished surface exhibited a groove height of 6.5 μm, whereas no discernible grooves following a pattern were observed on the polished surface, with a maximum peak-to-valley height of 2.5 μm. Both surfaces appeared flat, with a total vertical variation of 55 μm. Measured characteristic values of surface roughness parameters of the examined unpolished and polished interfacial surfaces are presented in Table 3. The mean roughness height, S_a , was found to be higher by a factor of 1.5 in the case of an unpolished surface. The mean spacing between the peaks, S_m , indicates that the grooves originating from the peeling-created valleys were approximately 30% wider. Higher peaks combined with wider valleys led to an eight-fold increase in the surface material volume, S_{mv} (the amount of material contained in the surface peaks). The process of polishing the cable resulted in a uniform surface with a quantifiable degree of roughness at its interface between the cable and the SOT.

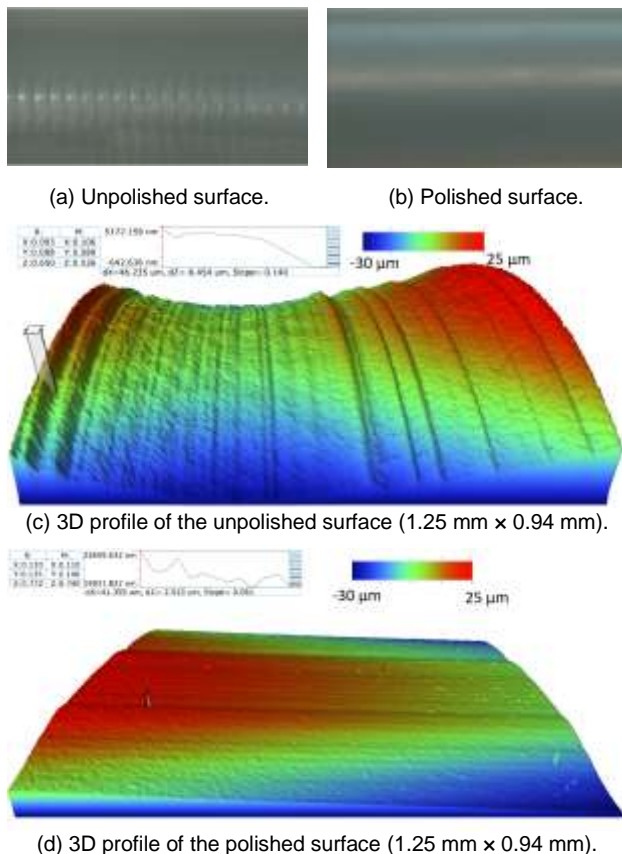


Fig. 3: Pictures and surface profiles of the-XLPE cable after peeling and polishing.

Table 3: Measured characteristic values of surface roughness S-parameters of the examined unpolished and polished cable surfaces.

	S_a [μm]	S_m [μm]	S_{mv} [nm ³ /nm ²]
Unpolished	14.1	47.1	480
Polished	9.2	31.1	60

PD measurements

Table 4 summarizes the PDIV (and PDEV values in parenthesis) obtained for test objects subjected to three different interfacial pressures and assembled using two different lubricants. PDs were detected at or above U_m of the SOT (24 kV) in all cases. For test object no. 3, PDs initiated 33% above the U_m of the SOT. The measured PDIV of test object no. 1 (baseline case) was by far the highest (56 kV) of all test objects. Hence, in the following investigations, it was assumed that all the PDs detected in the remaining consecutive cases originated from the cable end, where the SOT was replaced with an unused one for each pressure-lubricant combination.

The PDIV values for the SOTs installed using silicone grease were 33-65% higher than those installed with synthetic ester, with the discrepancy becoming more pronounced as external pressure increased. Moreover, when high external pressure was paired with the synthetic ester (test object no. 4), it resulted in only a marginally higher PDIV (2 kV) compared to the reference case where no external pressure was used with silicone grease (test object no. 3). The trend of PDEV followed that of PDIV in each case such that higher external radial pressure applied on the SOT also resulted in increased PDEV values, as demonstrated in Table 4.

Table 4: PDIV (and PDEV) values of the SOTs installed with different lubricants and at various pressures.

PDIV (PDEV)	No Pressure [kV]	Medium Pressure [kV]	High Pressure [kV]
Sil. grease	32 (22)	40 (26)	56 (32)
Synth. ester	24 (14)	28 (14)	34 (16)

Fig. 4(a) and (b) demonstrate PD repetition rates per period at different PDIV values under three different pressures for the lubricants grease and ester, respectively. For the PD magnitudes between 0.8 - 8 pC, similar pulse repetition rates were observed for the ester, regardless of the applied external pressure. However, a slightly higher repetition rate was detected at higher external pressure values for the grease, as displayed in Fig. 4(a). On the other hand, for pulse magnitudes beyond 7 - 8 pC, the repetition rate decreased in the case of medium pressure for both lubricants, where the magnitudes did not exceed 20 pC. This drop was more pronounced for ester, as shown in Fig. 4(b). For both lubricants, PD magnitudes beyond 20 - 22 pC were only observed under high external pressure, with very similar repetition rates. The only notable difference was that pulses larger than 37 pC, exhibiting a significant repetition rate, were only observed in the case of silicone grease under high pressure.

PRPD plots, as shown in Fig. 5, follow typical PD patterns originating from cavity discharges [12], [13]. Each PRPD plot incorporates all discharge events that took place during

the 5-min recording at the corresponding PDIV value with densities represented by the color bars on each figure's right side. PD magnitudes did not exceed 100 pC in all cases; thus, the voltage at the PDIV was kept for the entire duration. Although PD pulse distributions were symmetrical in both half-cycles in all cases, the density and the shape of the PD clusters seemed to differ as a function of the applied pressure and lubricant type. 'Rabbit ear-shaped' clusters were predominant when grease was used as the lubricant under no-pressure and medium-pressure conditions. In the case of high pressure, these 'rabbit ear-shaped' clusters transformed into 'tortoise-like' clusters. As for the synthetic ester, 'tortoise-like' clusters were the dominant pattern across all pressure levels, with noticeable 'rabbit ear-shaped' clusters subtly discernible under medium pressure. To elaborate on this, PD quantities were extracted from the raw PD data (up to the 99.9th percentile).

Fig. 6(a) displays the sum of the absolute values of the apparent charges for all PD events occurring within a single voltage period. For the synthetic ester, an insignificant increase was observed (<1%), while for the grease, discharge magnitudes increased more than three times under high pressure. A similar trend was noted for the total number of PD pulses that occurred during the 5-min recording period (15,000 AC cycles), as demonstrated in Fig. 6(b). In the case of synthetic ester, a slight increase of 15% in the number of PD pulses was seen under high pressure compared to the no-pressure case. Conversely, for the grease, the number of PDs increased to 1.7 times under medium pressure and 4.6 times under high pressure, compared to the reference case (no pressure).

The highest discharge magnitude was recorded under high pressure for both lubricants, as presented with the error bars in Fig. 6(c), where the electric stress was the highest. There were no significant differences between the maximum discharge magnitudes for both lubricants under no pressure and medium pressure.

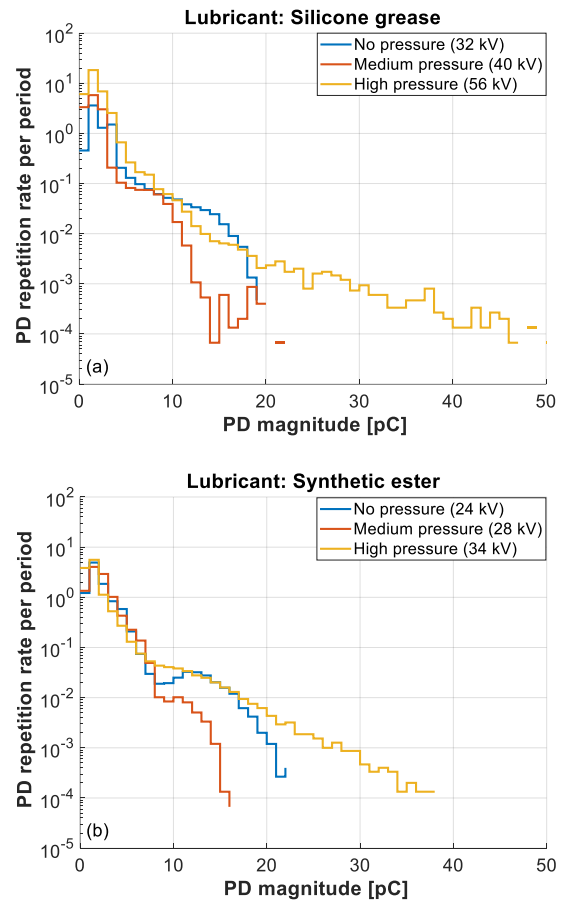


Fig. 4: PD repetition rate per period at PDIV under three different pressures with lubricants: (a) Silicone grease. (b) Synthetic ester.

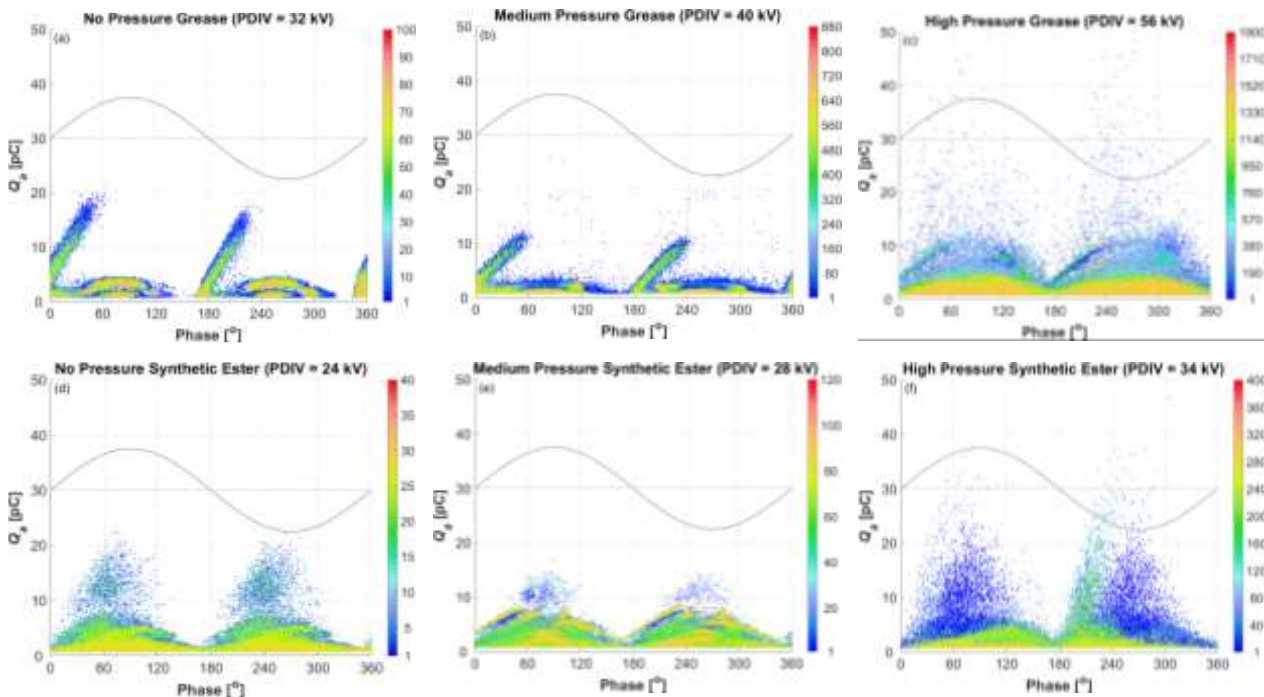


Fig. 5: PRPD ($Q_a - \phi - n$) plots incorporating PD pulses up to the 99.9th percentile during 5-min recording. Silicone grease: (a) No pressure at 32 kV. (b) Medium pressure at 40 kV. (c) High pressure at 56 kV. Synthetic ester : (d) No pressure at 24 kV. (e) Medium pressure at 28 kV. (f) High pressure at 34 kV.

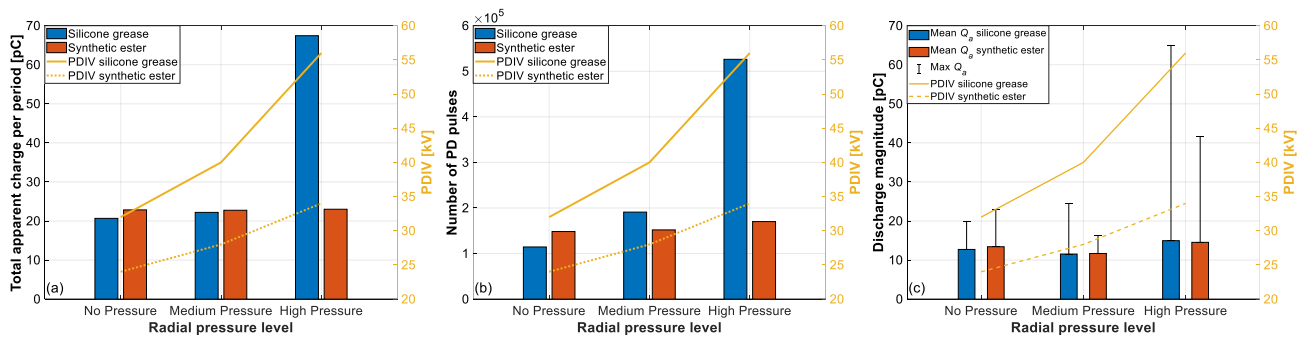


Fig. 6: Extracted PD quantities at the PDIV value for each case: Left y-axes represent the bars, whereas the right y-axes represent the PDIV shown by a line for each lubricant. (a) Total apparent charge per period. (b) Number of PD pulses. (c) Mean and max discharge magnitude (mean calculated for discharges above a 10-pC threshold).

Adopting a PD threshold of 0.8 pC, as was done for the other PD quantities, the mean discharge magnitude ranged between 2 - 3 pC in all cases. This can be attributed to the significantly higher numbers of discharges smaller than ~10 pC compared to those at higher magnitudes, as shown in Fig. 4. To investigate potential variations in the mean discharge values as a function of pressure and lubricant type, a PD threshold of 10 pC was applied to the raw PD data. Mean values were subsequently calculated (see Fig. 6(c)). Despite this, the mean discharge magnitudes remained low in all cases, ranging between 11 - 15 pC. A slight reduction under medium pressure for both lubricants was noted, aligning with the trends observed in the PD repetition rate (Fig. 4) and PRPD plots (Fig. 5).

DISCUSSION

Clear differences in PD quantities and patterns were observed between the test objects. Additional external pressure applied using IV tape caused the SOTs to deform both in radial and axial directions, as illustrated in Fig. 7. While wrapping the IV tape, the SOT was fixed at its original central axial position. Under medium pressure, there was an axial extension of 9%, further increasing to 19% under high pressure. The external pressure applied by the nominally stretched IV tape did not significantly deform the SOT under medium pressure. Conversely, the SOT experienced a substantial axial extension under high pressure due to the significant external pressure applied to the rubber material. As the radial diameters included six layers of IV tape with different thicknesses due to different stretching, the resulting radial deformation could not be detected accurately by simply measuring the outer diameter change.

Accurate estimations of the stresses and pressure in deformed/compressed materials can be calculated from deformation measurements. This would involve calculating the deformed volume using the dimensions provided for each case. The material properties from tensile and compressive measurements of both the rubber and the field-grading material of the SOT should also be determined. These data could then be utilized to estimate the displacement and elongation using models such as Neo-Hookean, Mooney-Rivlin, Yeoh, and Ogden [14]. From this, an estimation of the radial interfacial pressure can be performed. However, such detailed quantifications will be focused more closely in a follow-up study.

The solid-solid interface between the cable and the

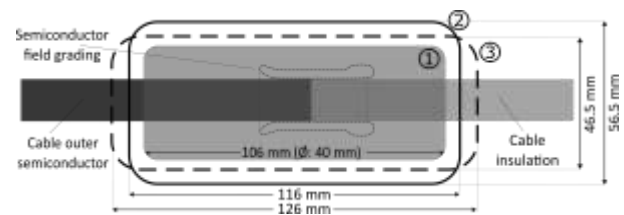


Fig. 7: Illustration of the SOTs under three different pressure levels (to-the-scale): 1: No pressure (as-is). 2: Medium pressure (including the IV tape layers). 3: High pressure (including the IV tape layers).

geometric field grading rubber material of the SOT comprises a system of sub-micro cavities and channels. These gaps are either filled or partially filled with the lubricant used during installation. Our earlier study [7] employed a data-driven deterministic approach to model solid-solid interfaces. This approach suggests that the number of enclosed cavities can significantly increase at an interface that combines soft materials, very high contact pressure, and smooth surfaces. Conversely, the model also suggests that interfaces involving hard materials, rough surfaces, and low interfacial pressure likely consist mostly of vented channels. It is important to note that the model only accounted for dry conditions without the inclusion of any lubricant. Consequently, the morphological changes in the presence of a lubricant may exhibit some variation. Based on these premises, considering the significant deformation observed in the SOT, especially under high pressure, it is plausible that a greater number of contact spots were formed. This, in turn, likely resulted in smaller microcavities and channels. The possible structural changes resulting from an increase in radial pressure should be considered along with the effect of the viscosity of the lubricant to be able to explain why the PRPD patterns, PDIV values, and PD quantities were different for silicone grease and synthetic ester under the same interfacial pressure and surface roughness.

At the microscale, the extent to which lubricants effectively 'wet' solid surfaces is not known. Wetting of surfaces depends on the properties of the surfaces and lubricants. Non-uniform lubrication can result in the formation of dry areas containing microcavities. Moreover, the increased interfacial pressure can cause the excess lubricant to form thinner layers and fill partially filled microcavities more effectively. However, if the lubrication is non-uniform and inadequate, external interfacial pressure can cause the

lubricant to be expelled from certain cavities, leading to the coexistence of larger air-filled and lubricant-filled cavities/channels at the interface. The uniformity of the surface lubrication and the amount of lubricant removed from microcavities are strongly dependent on the viscosity of the lubricant and the applied pressure level. Sections of dry contacts may have also caused local buckling at the interface leading to air-filled gaps [3].

Synthetic ester likely exhibits minimal distribution changes when the pressure is increased. This could be a reason for the limited changes observed in the PDIV values, PRPD patterns, and PD quantities for the synthetic ester. In contrast, silicone grease could expand further under higher pressure, allowing excess grease to fill empty (only air-filled) and partially filled microcavities more effectively. This could explain the more pronounced differences observed in the PDIV, PRPD patterns, and PD parameters for the grease as the pressure was increased. Especially under high pressure, PRPDs changed from 'rabbit ear-like' to 'tortoise-like' patterns, suggesting that grease expanded and filled empty or partially-filled channels and was probably homogeneously distributed at the interface. More microcavities could be discharged due to the increased electric field at a higher PDIV. PD-induced hot electrons could mechanically displace the grease and thus create cavities at a micro-scale. While increased electrical stress can enhance the bombardment of hot electrons, higher pressure could impede this mechanism. This could perhaps explain the disappearance of 'rabbit ear-shaped' PRPDs at high pressure.

CONCLUSIONS

From this study, it can be concluded that:

- Increasing the total radial pressure beyond the level obtained when expanding the SOT on the cable core resulted in higher PDIVs independent of the lubricant type.
- Significant differences in PRPD patterns at PDIV were observed for silicone grease and synthetic ester, suggesting sub-micro morphologies of the lubricated interfaces are different.
- It is likely that the higher viscosity of the lubricant increased the PDIV of the SOT at the same interfacial pressure and surface roughness.
- To avoid plastic deformation of the insulating and semi-conductive rubber materials in the termination when applying external radial pressure, both modeling and measurements of the resulting hoop and radial stresses should be conducted.

Acknowledgments

We would like to express our gratitude to the LowEmission Centre (<https://www.sintef.no/projectweb/lowemission/>) and FME NorthWind (<https://www.northwindresearch.no/>) for their support.

REFERENCES

- [1] E. Gulski *et al.*, 'Discussion of electrical and thermal aspects of offshore wind farms' power cables reliability', *Renew. Sustain. Energy Rev.*, vol. 151, p. 111580, Nov. 2021, doi: 10.1016/j.rser.2021.111580.
- [2] D. Kunze, B. Parmigiani, R. Schroth, and E. Gockenbach, 'Macroscopic internal interfaces in high

- voltage cable accessories', in *e-cigre*, 2000. Accessed: Apr. 26, 2023. [Online]. Available: https://e-cigre.org/publication/15-203_2000-macroscopic-internal-interfaces-in-high-voltage-cable-accessories
- [3] B. Bhushan, 'Contact mechanics of rough surfaces in tribology: multiple asperity contact', *Tribol. Lett.*, vol. 4, no. 1, pp. 1–35, Jan. 1998, doi: 10.1023/A:1019186601445.
- [4] Z. Li, K. Zhou, X. Xu, P. Meng, Y. Fu, and Z. Zeng, 'A Thermal Excitation Based Partial Discharge Detection Method for Cable Accessory', *IEEE Trans. Power Deliv.*, pp. 1–8, 2023, doi: 10.1109/TPWRD.2023.3254907.
- [5] R. Ross, 'Dealing with interface problems in polymer cable terminations', *IEEE Electr. Insul. Mag.*, vol. 15, no. 4, pp. 5–9, Jul. 1999, doi: 10.1109/57.776938.
- [6] E. Kantar, F. Mauseth, E. Ildstad, and S. Hvidsten, 'On the tangential AC breakdown strength of polymer interfaces considering elastic modulus', in *2017 IEEE Conference on Electrical Insulation and Dielectric Phenomenon (CEIDP)*, Oct. 2017, pp. 816–819. doi: 10.1109/CEIDP.2017.8257567.
- [7] E. Kantar and S. Hvidsten, 'A deterministic breakdown model for dielectric interfaces subjected to tangential electric field', *J. Phys. Appl. Phys.*, vol. 54, no. 29, p. 295503, May 2021, doi: 10.1088/1361-6463/abfbaf.
- [8] E. Kantar, 'Longitudinal AC Electrical Breakdown Strength of Polymer Interfaces: Experimental and theoretical examination of solid-solid interfaces considering elasticity, surface roughness, and contact pressure', NTNU, 2019. Accessed: Nov. 05, 2019. [Online]. Available: <https://ntnuopen.ntnu.no/ntnu-xmlui/handle/11250/2606181>
- [9] 'MIDEL 7131 biodegradable synthetic ester transformer fluid', *MIDEL*, Jun. 01, 2019. <https://www.midel.com/app/uploads/2018/05/MIDEL-7131-Product-Brochure.pdf> (accessed May 14, 2023).
- [10] NKT GmbH, 'Product information for assembling paste MV3 for cable accessories 21527-35'.
- [11] Z. Li *et al.*, 'Morphology evolution and breakdown mechanism of cross-linked polyethylene (XLPE)–silicone rubber (SiR) interface induced by silicone grease diffusion', *High Volt.*, vol. 7, no. 4, pp. 802–811, 2022, doi: 10.1049/hve2.12176.
- [12] J. Fuhr, 'Procedure for identification and localization of dangerous PD sources in power transformers', *IEEE Trans. Dielectr. Electr. Insul.*, vol. 12, no. 5, pp. 1005–1014, Oct. 2005, doi: 10.1109/TDEI.2005.1522193.
- [13] L. Wang, A. Cavallini, G. C. Montanari, and L. Testa, 'Evolution of pd patterns in polyethylene insulation cavities under AC voltage', *IEEE Trans. Dielectr. Electr. Insul.*, vol. 19, no. 2, pp. 533–542, Apr. 2012, doi: 10.1109/TDEI.2012.6180247.
- [14] G. A. Holzapfel, *Nonlinear Solid Mechanics: A Continuum Approach for Engineering*, First Edition. Chichester ; New York: Wiley, 2000.

GLOSSARY

- IV tape:** Insulating vulcanization rubber tape
PD: Partial discharge
PDIV: Partial discharge inception voltage
PDEV: Partial discharge extinction voltage
SiR: Silicone rubber
SOT: Slip-on termination
XLPE: Cross-linked polyethylene